International Journal of Advanced Engineering Research and Science (IJAERS)
Peer-Reviewed Journal
ISSN: 2349-6495(P) | 2456-1908(O)
Vol-8, Issue-8; Aug, 2021
Journal Home Page Available: https://ijaers.com/
Article DOI: https://dx.doi.org/10.22161/ijaers.88.32

# Remote Sensing for Risk Mitigation in Agricultural Financings: Multitemporal Change Detections in Agricultural Areas using the Delta NIR and Delta NDVI Models

Sumaia Resegue Aboud Neta, Edilson de Souza Bias

Institute of Geosciences, National University of Brasilia, Brasilia, DF, Brazil.

Received: 09 Jul, 2021,
Received in revised form: 10 Ago, 2021,
Accepted: 14 Ago, 2021,
Available online: 22 Ago, 2021

***Keywords*— Delta NDVI, Delta NIR, LimiariZC, Nanosatellites, Python, Remote Sensing.**

***Abstract*—** *Agribusiness is one of the main pillars of the world economy, where the agriculture sector is fundamental to the economy of countries and contributes strongly to poverty reduction, positive balance of trade and inflation control. The countries have government policies that subsidize agricultural credits with low financing rates in order to encourage the sector. With the expansion of agricultural areas to meet the growth in the world population, its necessary a technological revolution in the field, as is increasingly necessary to mitigate risks in the financeable area, with quick and transparent inspection. Thus, a tool in Python language was develop containing a methodology for monitoring the cycle of cultivation in agricultural areas with emission of alerts messages in cases of deviations in the behavior of the planted area. Delta NDVI and Delta NIR models were developed to monitor agricultural cycle and were able to perform remotely the multitemporal detection of changes. The study was in an area in Brazil, using 9 images from the Nano Satellite Planet, from 2017 to 2019. The results were assertive, because the classifications of methods detected changes in the patterns of agricultural, emitting signals in cases of deviation from behavior with alerts for loss of vegetation from initial cycle, full and final of maturation. As the variation between models was not expressive, Delta NIR was an attractive alternative for change detections because uses only one band, the processing is less costly, with low response time and good performance, with execution in less than half time. Thus, the models were assertive and can facilitate inspection by of the countries with subsidies for agriculture, whether by inspectors from the Government or by Financial Institutions, in addition to reducing costs in the operational process concentrating visits only for areas of large hectares.*

## I. INTRODUCTION

Agribusiness is one of the main pillars of the world economy. The importance of the sector goes beyond the food factor, where agriculture is one of the main responsible for the positive balance of trade in several countries. Thus, the agriculture sector is fundamental to the economy of developing countries, where the agricultural progress contributes strongly to poverty reduction [3] [45].

According by [61] there has been a significant growth in the world population, where by 2050 60% more food, 50% more energy and 40% more water will be needed to

supply the consumption of the planet's population. In the 1950, a world population was 2.6 billion people, having increased to 5 billion in 1987, 6 billion in 1999 and 7 billion in 2011. For the next 30 years, there is an expectation of an increase of 25%, around 2 billion people, with a forecast of 9.7 billion in 2050, with 70% of the urban population having higher income levels than today. For the 2100 year, predictive scenarios indicate an increase of around 43% in the world population, totaling 11 billion people. Thus, it has been observed that after the Industrial Revolution, the population has grown exponentially, which has resulted in a greater demand for food with the need for technologies to reduce costs and expand opportunities, making it increasingly necessary to digitize the field with productivity gains in a sustainable way [1] [28] [60] [61].

According by [59], 85% of the global growth of agricultural production in the coming years will be due to improvements in the production process, such as better use of inputs, investments in technology and better cultivation practices. Therefore, the digital revolution in the countryside will bring greater intensification of land use, where scenarios indicate that the expansion of agricultural area will be only 5%, improving the productivity and sustainability of agriculture, doing more with less.

There are few countries that still have uncultivated areas that can be used for agriculture, with 90% of them in South America and Africa. However, most countries do not have technologies for production in uncultivated areas, in addition to the lack of qualified professionals and economic resources. Given this scenario, the medium and long-term perspectives, they place Brazil as an important global producer to supply as business opportunities and responsibilities in the production and supply of food in the world. Currently, only 34% of its area is used in agribusiness (with 23% in agriculture and 77% in pastures) and has around 49% in forests or protected areas. Still, it participates with only 4% of the world trade in agribusiness and can supply a portion of the future world demand for food [74].

Brazil is the 4th largest grain producer in the world (rice, barley, soybeans, corn and wheat) accounting for 7.8% of world production and only behind China, the USA and India. Furthermore, it is the 2nd largest exporter of grains, with 19% of the international market, in addition to accounting for around 50% of the world trade in soybeans. In relation to grain, Brazilian exports totaled US$ 30 billion in 2020, and US$ 346 billion in the last two decades [27].

The Brazil concentrates around 14% of the world's fresh water, is a country with a diversified climate and regular rainfall, in addition to having a value close to 400 million hectares (ha) of fertile agricultural land, it has in agribusiness a pillar for expressive growth of the economy. In the last decades, agricultural areas in the country have grown, due, in large part, to the increase in the regions of pastures and expansion of soy and sugar cane [54] [65].

Brazil is one of the main producers of agricultural commodities in the world, and agribusiness is considered one of the most important sectors of the Brazilian economy, representing almost a quarter of all national production. In 2019, the sector's share of the economy's total Gross Domestic Product (GDP) was 21.4%, having contributed over the years to the trade balance and inflation control [10] [29].

In recent years, the sector has seen an increase of around 110% in Government Federal investments, from 107.2 billion in the 2011/2012 harvest to 225.59 billion in the 2019/2020 harvest [53]. Because it is a dynamic sector and due to its capacity to promote other areas, agribusiness occupies a prominent position in the global scenario, having an increasing importance in the economic development process. In general, there are several lines of investment and financing focused on agriculture, from costing to marketing, involving the entire production cycle. According to data from the Confederation of Agriculture and Livestock of Brazil (CNA) and the Centre for Advanced Studies in Applied Economics (CEPEA), in 2019 there was an increase in the GDP of Agribusiness by 3.81%, meeting the projection of the National GDP that growing 1.1% in 2019, this being the smallest advance in the last three years. Thus, if it were not for Agro growth and Government Federal investments, could be a retraction in the economy in the country [10].

For the coming years, the predictive scenario indicates an increase in federal incentives, in view of a harvest forecast for 2028/2029 with an increase of close to 45% in grain production. The perspective contemplates the production and development dimension of planted areas considering the fifteen products surveyed monthly by CONAB in crop surveys [53]. Brazil is the second world exporter of soybeans and among Brazilian regions, the Midwest accounts for more than 42% of the country's total production, with approximately 90 million grains - including cereals, legumes and oilseeds - followed by the South region with production around 35%, Southeast with 10 %, Northeast 9% and 4% of the North region [15] [33] [40].

Soy, corn and rice are part of the so-called Annual Cycle, or short-cycle crops, whose periodicity of the production cycle is completed in a period of one year or less, with the need for new planting after harvest. In addition to the crops mentioned, annual crops include

peanuts, wheat, beans, cassava, sugar cane, barley and sunflower. Also, in the category are fruit and vegetable production, such as melon, papaya, watermelon, potato, tomato, onion, carrot and garlic, which have short development cycles with several harvests throughout the year, being the Brazil is the third world producer in the segment, behind China and India [8] [15] [26].

As agribusiness is important in the world economy, whether due to the surplus in the balance of trade or inflation control, not only Brazil bus the most countries have government incentives in the sector through agricultural credits released by Banks and Financial Institutions. This rural credit is financing for rural producers whose activities involve the production and/or sale of products in the agricultural sector. Thus, governments attach great importance and support to agricultural development through financial investments [62] [79] [84].

Countries such as Egypt, Morocco, Nigeria and South Africa have strategic government policies for agricultural financing in emerging markets [62]. On the European continent, countries like Serbia have strict rules for releasing bank credits for agricultural financing and have state support. Loans are subsidized by the Ministry of Agriculture and since 2004 they have been supported by banks with low interest rates. In 2017, the budget for agriculture represented 4.78% of the planned budget revenues of the Republic of Serbia [79]. In France, the government adopted a series of measures to accelerate agricultural development through Financial Agencies aimed at agricultural policies with national financial incentives, where support for agricultural credit played an important facilitating role in agricultural modernization in France. In Japan, government subsidy investment in agriculture has increased in recent years, which plays an increasingly significant role in agricultural development. The Japanese government has issued several financial policies and regulations to strengthen Government support in agriculture and to regulate the sector's investment policies [84].

In view of this scenario, with the increasing evolution of public incentives and investments in the agricultural sector in different countries, in addition to the significant importance in the GDP of the economy, it is necessary to have risk mitigators in the financeable area in order to monitor agile and efficient manner the reality of agricultural areas, where many of the agricultural practices end up having financing through the National Financial System of countries sponsors.

Proof of this is the recommendation of the Brazil Central Bank (BACEN) for Banks and Financial Institutions, liable to rural credit operations, to make use of Remote Sensing to contract and inspect agricultural operations credit operations [4]. Although there have been some advances in recent years, such as the inclusion of UAVs (Unmanned Aerial Vehicles) for monitoring agriculture, the inspection methods are almost entirely in loco, which makes monitoring costly and often with reactive actions and not the proactive actions on the verge of eventual problems. Thus, a tool in Python language was developed, called LimiariZC, where modules was developed with the objective of to propose a method for detecting changes in agricultural areas, with automated emission of messages for cases in which behavior change is detected, using models of seasonal differences bitemporal through Delta NIR and Delta NDVI, thus contributing to risk mitigators in the financeable area and remote inspection instead of in loco, with the possibility of quantifying areas of anomalies as well as analyzing the vegetative cycle of the crops. Thus, the methodology aims to monitor the development of cultures, reducing face-to-face work. The models were applied in a study area in Brazil but can be used in any region of the planet for monitoring areas with agricultural financing or that will be financed and thus have greater control.

## II. THEORETICAL REFERENCE

### 2.1 Change Detection

According by [52], the change detection can be defined as changes that occur over time on the Earth's surface, where comparisons are made between images obtained at different times. The monitoring of these changes can be performed using visual and / or digital analysis techniques, using multitemporal data, by Remote Sensing systems [6] [11].

In the study by [51], the diversity of change detection techniques developed in the last decades is demonstrated, mainly due to technological advances. Thirty-one change detection practices grouped in a macro way into seven categories were presented: Algebra (including different algebraic operations), Transformation (with Principal Component Analysis and Chi-Square, reducing redundant data), Classification (concentrating post- classification, spectrum, hybrid detections and neural networks), Advanced models (such as reflectance, spectral mixing and biophysical parameter estimation models), GIS (GIS-based change detections), Visual Analysis (includes visual interpretation of the operator in multitemporal images as well as the digitization of areas of change) and Other techniques (which do not fit into the previous six categories). However, several studies and authors

corroborate that there is no method capable of solving all problems [25] [51] [81].

To [3], carried out a study to detect changes in forest degradation by mining trajectories in the land cover, and through the monitoring and characterization of forest changes it was possible to map the environmental and social processes that influenced the changes. The model was developed in C ++ language using the free TerraLib library [9], where four grouping classes were defined, the methodology being applied in a region located in the state of Pará, in the Amazon Biome, in Landsat images 5. The results showed that it was possible to infer that as forest degradation is a dynamic and long-term process, it is necessary to have at least data with annual intervals for assertive detection, with the proposed model being effective in characterizing the trajectories of changes.

[39] used NDVI time series, extracted from Sentinel-2A for monitoring and detection of sugarcane management zones in a region located in the interior of the state of São Paulo. Six different dates from the satellite were analyzed, where it was found that there was spatial dependence on the vegetation indices in all scenes. The analyzed method allowed, through the interpolation of NDVIs, to delimit different management zones in addition to the vegetative development cycle of sugarcane, having been assertive in the monitoring and detection of agricultural practices.

[14] made use of a Nano Satellites Planet time series for monitoring and detection in an indigenous village in Rio Grande do Sul, where the results indicated lower values of environmental degradation compared to regeneration, indicating a conservation trend in the region.

In [67], change detections in land use and cover and landscape fragmentation were monitored in a region located in Western Bahia, over a period of ten years. ALOS and Landsat-5 images were used where it was found that in the period studied, agriculture and livestock grew over 200%, while natural vegetation decreased by around 26% in the region.

In the work presented by [77], a change detection technique with predictive analysis on land use and land cover in the Pantanal region was demonstrated. The methods were classified by object-oriented analysis where, using the Hierarchical Process combined with Markov Chain and Cellular Automata, a predictive detection scenario was generated until the year 2050. The multitemporal analysis indicated a tendency to reduce natural areas, such as vegetation and water bodies, with increased grazing areas and exposed soil, indicating possible degradation of the Pantanal landscape.

In the midst of different studies and techniques for detecting changes, in recent years the use of deep learning and machine learning has become popular, mainly for recognizing patterns in the medical field. As an example, the techniques have supported automated diagnoses on radiographs, as in the analysis of pneumonias, serving as a possible basis for further identification by Covid-19 [46] [75] [78]. However, for the effective assertiveness of models, monitoring and detections, there is a need for a significant volume of data for training and consequent quality of detection. Thus, in view of different techniques, the method must be selected according to the appropriate approach in solving the study problem [48] [85].

In view of the different techniques, particularities and technological developments, the monitoring of agricultural crops - whether for estimating and forecasting crops with different crops, for different climatic conditions or for computational tools - represents a challenge to entities related to the agricultural sector and official bodies governmental organizations, such as IBGE and CONAB [16] [41].

In the literature, techniques for detecting changes in land use and land cover are preferentially categorized in terms of their use, usually belonging to two categories: one relating to the monitoring of incremental and decremental change processes, such as multitemporal analysis and time series work [38] [71] and another related to comparative analyzes, focused on dynamic and cyclical changes, such as studies in relation to planted area and crop comparisons [20] [58].

Over the past few decades, different studies and agro-environmental monitoring programs have emerged, with different methods involving the production cycle, from predictions of planted area estimates, pest monitoring to predictability of productivity for agricultural areas. Among the programs presented to the scientific and academic community, are the GeoSafras and SigaBrasil projects, coordinated by CONAB [37]. It is also worth mentioning RadamBrasil, which was the first government initiative in monitoring and mapping vegetation in the country and aimed at mapping mineral resources, vegetation and soil cover. The project focused on the Amazon region and the Northeast, being conducted between 1975 and 1980 using airborne radar images, where there was an onerous effort in the visual interpretation of information [19].

The National Institute for Space Research (INPE), in conjunction with the Ministry of Science and Technology (MCT), coordinates the CanaSat project, which since 2003 has been monitoring the annual growth of sugarcane cultivated areas in the south-central region of Brazil, through images from the Landsat, CBERS and Resourcesat-I Satellites [43] [73].

The Anti-rust Consortium has an Alert system for monitoring soybean crop, where it monitors the dispersion of the fungus that causes Asian rust. The alert system arose due to the need of farmers and entities linked to agricultural practices for a tool that would alert the rural community in a practical and efficient way regarding the occurrence of pests in crops in order to mitigate the spread of the disease [37] [56].

Through Project MARS (Project Monitoring Agriculture with Remote Sensing), crop monitoring and crop estimates have been carried out in the scope of the participating states of the European Union. The information is extracted from the combination of agrometeorological models, a trend function with technological improvements and spectral data, through NOAA / AVHRR and SPOT / VGT images [21].

The European Environmental Agency, in conjunction with Research Centers, launched the CORINE program (Coordination of Information on Environment), with the aim of making an inventory of the physical environment and soil cover in Europe, through 44 classes with a minimum mappable of 25 ha using Landsat-5/7/8, SPOT 4/5, IRS P6 LISS III, Rapideye and Sentinel-2 images. Monitoring has been carried out over the last few decades, and in 2018 the thematic accuracy extracted was over 85%, considering 39 countries involved in monitoring [2] [21] [30].

Different crop monitoring and detection solutions have emerged in recent years, aiming to find methods and alternatives to solve particularities of agribusiness as technological evolution and digital transformation progressed. Thus, there is a growing trend in the implementation of methods, models and Agro-Environmental monitoring programs. According to data from the United Nations (UN) for food and agriculture, there is an expectation of a 70% growth in agricultural production for the next decades. Therefore, the processes related to the monitoring of agriculture will need to be increasingly productive and efficient, with the innovation of technological means to monitor agricultural practices [23].

### 2.2 Anomaly Models: Delta NIR and Delta NDVI

In the monitoring of vegetation, in a healthy foliage there is expressive reflectance in the region of the Near Infrared (NIR), with significant spectral response also in the Green band of the visible, in comparison with the bands in the wavelength of Red and Blue. Thus, the analysis becomes a strong indicator of the stage of development of the culture. In stressed foliage, there is a significant reduction in reflectance at NIR, approaching reflectance at Green. In general, stress is caused by water scarcity, exposure of exposed soil to deforestation and degradation of vegetation. In dry foliage, however, the spectral responses of the visible and infrared bands become very close [63].

Over the years, more than 50 indexes used in monitoring vegetation have been proposed, one of the most used being the Normalized Difference Vegetation Index (NDVI) [44] [55].

NDVI is an index of significant importance in the characterization of vegetation, where from satellite images it is possible to enhance vegetation by mathematical operations between the bands of the sensor satellites. Thus, the index assists in estimating biomass, carbon sequestration by vegetation, vegetation cover and in detecting changes in land use and land cover patterns, by monitoring seasonal dynamics [32] [76].

The NDVI calculation is performed from the ratio between the difference in the reflectance of the near and visible infrared bands with red, by the sum of the reflectance of these bands, according to Equation 1 [44]:

$$NDVI = \frac{(NIR - RED)}{(NIR + RED)} \qquad (1)$$

The index represents the normalized magnitude that varies between -1 and +1, resulting from the difference between the reflectance of the spectral bands. Thus, the closer to the value 1, the greater the probability of the presence of vegetation. The closer to -1, the greater the indication of the presence of exposed soils and rocks in the analyzed area [44] [76].

In the Fig. 1, it is presented in (a) the reflectance of the vegetation in the bands of the electromagnetic spectrum for healthy, stressed and dry vegetation. In (b) the approximate emission percentages for healthy and dry vegetation.

In annual crops, there is a standard profile in which the NDVI values show low initial values in the initial vegetative cycle (similar to the exposed soil values) being increased as the plant grows due to the increase in biomass. Thus, with the full development of the crop, where there are characteristics of dense vegetation and in good water conditions, agricultural practice reaches the highest NDVI value. From then on, due to the reduction of vegetative vigor in the plant, the maturation process, or senescence phase, begins, where the NDVI values regress to the initial level of exposed soil at the beginning of the cycle [22] [50].

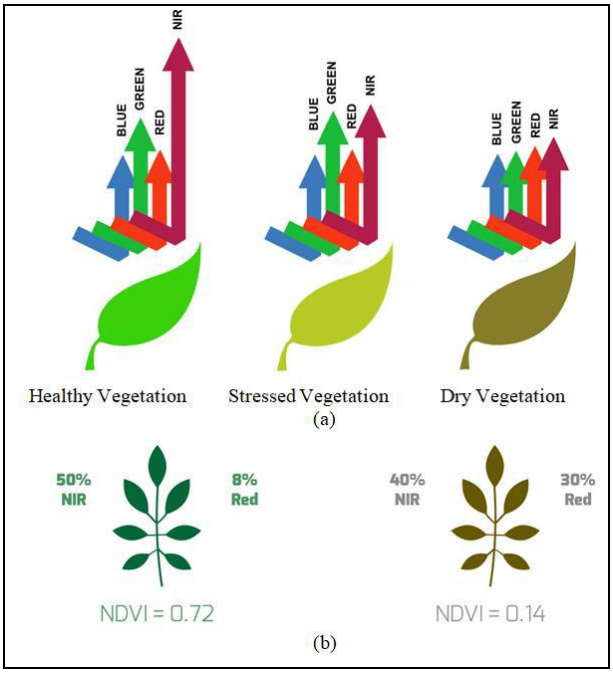


*Fig. 1: Different types Reflectances in the Vegetation Stages. Adapted from [63].*

In the visible red region, chlorophyll absorbs solar energy, causing low reflectance. In the near infrared range, both the internal morphology of the leaves and the structure of the vegetation, cause a high reflectance of the incident solar energy. Thus, the greater the contrast, the greater the vigor and incidence of vegetation in the imagined area [49].

According by [47], the NDVI index allows monitoring the amount of vegetation, and as there is an increase in vegetation in the green, there is an increase in the reflection of the near infrared band and a decrease in the reflection of the red band [64]. Thus, there is an increase in the ratio, expressed in Equation 1, enhancing the vegetation and making it expressive in the scene.

For [35], the NDVI index can be used to classify vegetation cover and map land use capacity. Still, there are studies that use the indicator for monitoring degraded areas, as well as for detecting environmental changes, as presented in the works by [66] [80]. In conjunction with geoprocessing tools and customized algorithms, it is also possible to perform the analysis of the temporal evolution of a given region, by comparing the current and past vegetation cover, thus estimating the percentage of devastated areas and being useful in monitoring activities photosynthetic, in addition to comparisons of seasonal and interannual variations [5] [69] [72].

In the Delta NDVI model, after extracting the NDVI from the input images, the algebraic subtraction operation is applied to the results of the NDVIs of the images, in order to find possible anomalies in the scenes by highlighting the differences. In Equation 2, the NDVI Delta is broken down, where the NDVI pixel by pixel is subtracted from the most recent image (NDVIMR) in relation to the NDVI of the oldest image (NDVIMA):

$$Delta\ NDVI = NDVI_{MR} - NDVI_{MA} \quad (2)$$

Similarly, in the Delta NIR model, pixel-by-pixel subtraction of the NIR bands is performed, with the most recent image (NIRMR) in relation to the oldest image (NIRMA), according to Equation 3:

$$Delta\ NIR = NIR_{MR} - NIR_{MA} \quad (3)$$

For the Delta NIR, the mathematical operation of the subtraction between the bands of the images can be performed through the different bands of the same image or the same band of different images, being useful to highlight small spectral nuances, reflected by the difference of the digital numbers of the scene. In multispectral images, the band difference can be used to characterize small differences in spectral behavior of certain targets. Still, it can be applied in the identification of different types of vegetation cover, amount of vegetation in the scene, in addition to detecting patterns of changes in soil cover [18].

For [44], in the generated difference images, the pixels in which there are intensities close to the average, identify areas without change detections. At the ends of the histograms, the pixels that had significant changes during the temporal evolution of the images will be concentrated. Still, there are studies that define a cut-off value, or threshold, for pixels as indicative of areas of change for each band in the difference image, as well as more refined parameters for monitoring changes [17].

Although simple, compared to other methods, the difference in bands makes it possible to monitor the loss of large vegetation with high precision. However, when there are differences in shading in the scene, caused by variations in lighting, or even the need for monitoring of undergrowth, where there are different soil moisture conditions, the detection may not be as accurate. Thus, it is possible to apply the method of differences on the transformed values of the original gray levels [47].

According by [17], of the techniques for detecting changes in land use and cover, image subtraction is one of the most used and with significant results. Still, the mathematical operations of subtraction and band ratio in multitemporal analyzes are widely used in the detection of deforestation and changes in land use [12].

For [49], the subtraction operation in the images allows to analyze the change in vegetation cover, or biomass

vigor between the images, and the higher the value in the difference image, the greater the increase in the representativeness of the photosynthetically active elements among the analyzed images, that is, of vegetation incidence. Thus, the greater the negative value in the regions, the greater the loss of vegetation. Regions with difference values close to zero, on the other hand, correspond to areas without significant changes.

For the Delta NDVI and Delta NIR models, in the histograms of the difference images, from the statistical analysis based on the values of minimum, maximum, mean and standard deviation of the subtraction image, it is possible to verify the oscillation of the standard deviation around average.

According by [57], when the difference in bands in wavelength ranging from 0.8 to 1.1 μm is used, changes to the standard deviation varying between 0.35 and 0.60 are detected. [24] values of 1σ indicate the anomalies detections, and the interpretation of changes will depend on the method used, the nature and the time scale used, as intra / interannual variations for the detection of seasonal differences in land use or for monitoring expansion of different agricultural practices.

In the Fig. 2 a Normal Distribution curve is shown, with mean (μ) 0 and standard deviation (σ) of 1, where the red and green highlights are respectively the explanations for negative anomalies (degradation of vegetation cover) and positive (regeneration of vegetation cover). The regions of the histogram with oscillation lower than -1σ around μ are called negative anomalies, while oscillations greater than + 1σ are considered as positive anomalies. The regions without significant changes in the comparison are called areas between anomalies, arranged between -1σ and + 1σ.

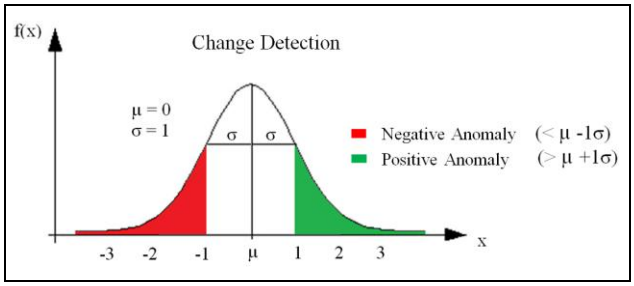


*Fig. 2: Change Detection with Negative and Positive Anomalies.*

By analyzing the results of extracting the attributes in the images, the knowledge model was defined so that rules could be established for detecting seasonal changes in the bitemporal analysis of the scenes, so that the multitemporal monitoring of changes was performed. Thus, it is possible to quantify the percentage of changes in vegetation loss between the scenes (negative anomaly) and consequently issue change signals from a maximum acceptable alert threshold stipulated, which can assume any value defined by the user. Because the objective of this study is to detect changes in the polygons / plots and not in the completeness of the scene, the threshold of 1σ around μ will be adopted for the change detections, according to the results described in section IV.

## III. MATERIALS AND METHOD

### 3.1 Study Area and Materials

The study region is concentrated in the eastern portion of the Federal District (DF) around the region called PAD-DF, the Federal District's Directed Settlement Program, close to the border of the state of Goiás in the municipality of Cristalina between latitude -16.09815 and longitude -47.47153, encompassing an area close to 70 hectares (ha), as shown in the Fig. 3.

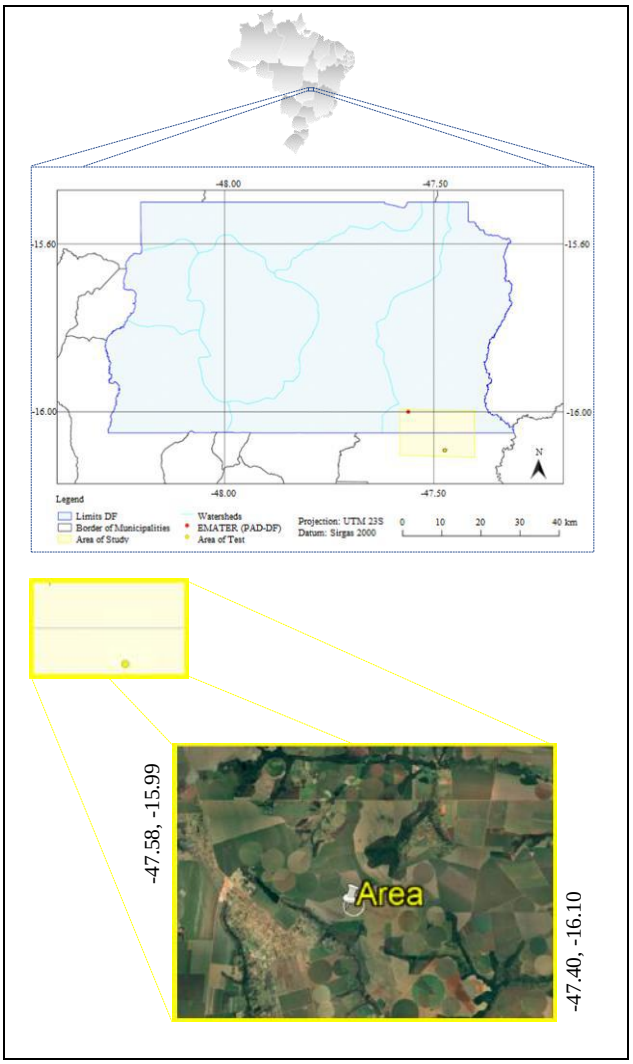


*Fig. 3: Study area around PAD-DF: Google Earth image from April 10, 2020.*

According to information from the Agricultural Census and Land Structure in the country [41] [42], of the total of 6.5 MM of rural properties, about 86.5% have less than 100 ha. Considering the DF dimension, the value rises to 94.3%. Thus, the dimension of the study polygon used in the application of the models, covers the largest number of Brazilian rural properties.

The polygon was chosen because it visually presents different nuances in the field throughout the monitoring of the culture development cycle. According to the field visit carried out on 10/23/2019, in the stand there is the diversification of Horticulture crops. In this way, the tests were applied to the polygon in order to analyze the use of the models for emitting signals in an automated way in the seasonal bitemporal variation of the scenes.

The PAD-DF is a program implemented in the 70s, with the purpose of leveraging agribusiness in the Brazilian Cerrado. The region covers more than 60 thousand ha, containing several types of economic initiatives and some of the main crops in the country, such as soybeans, corn, wheat, cotton, beans, onions, potatoes and carrots [7] [36].

For multitemporal monitoring of change detections, the monitoring of the agricultural development cycle in the field was carried out, where nine images of the Planet Nano satellite were used, as shown in Table 1.

*Table. 1: Images used for monitoring of the culture development cycle.*

| **Imagery Date** | | |
|---|---|---|
| **Nov 14, 2017** (Time: 12h45'10''; % cloud: 0%) | **Nov 28, 2017** (Time: 12h43'58''; % cloud: 0%) | **Dec 28, 2017** (Time: 12h45'48''; % cloud: 0%) |
| **Feb 14, 2018** (Time: 12h48'00''; % cloud: 0,16%) | **Apr 27, 2018** (Time: 12h50'43''; % cloud: 0%) | **Oct 04, 2018** (Time: 13h39'52''; % cloud: 0%) |
| **Jan 03, 2019** (Time: 12h52'13''; % cloud: 0%) | **Jan 15, 2019** (Time: 12h58'38''; % cloud: 0%) | **Feb 02, 2019** (Time: 12h58'55''; % cloud: 0%) |

The Planet images were defined as the scope of this work by the imaging characteristics of the nano satellites, with a significant daily and spatial temporal resolution of 3 meters, allowing for possible traceability needs of the plots with agricultural financing in an agile way, being essential for monitoring the vegetation cycle of the cultures. As the images are made available daily with repetition of the scenes by the sensor system, in case any abnormality is detected in the monitoring, it is possible to adopt timely actions in an agile and effective way, such as, for example, on-site inspection for the cases that were effectively carried out inconsistency is detected. Thus, it was adopted as a premise that the better the temporal spatial resolution, the better the monitoring.

The analysis and selection of the images were based on the criteria of availability of scenes, dates based on the phenological periods of the cultures present in the plot, the absence of clouds and visual inspection that indicated significant seasonal changes in the scenes, aiming to find periods with greater contrasts to assess the differences and consequently apply and validate the proposed methods with assertive signs for the cultures. The images used are the Analytical Ortho Scenes level 3B, which are made available by the supplier with geometric, radiometric, orthorectification corrections, in addition to being made available geo-referenced, normalized and scaled with Radiance at the Top of the Atmosphere (TOA), being delivered in the analytical products for the 4 bands (Red, Green, Blue, NIR) [68].

The applications QGIS 2.18 and Envi 4.8 were used respectively to cut the test areas in the images and validate the accuracy of the classifications performed in the tool developed in Pyrhon. Thus, the proposed methods were implemented in Python 3.6. The use of open source geotechnologies in this work, for data processing, has the purpose of minimizing costs, making the proposed methods of the Delta NIR and Delta NDVI models affordable, propagating their use, making possible the technical financial viability of research, in addition to have a wide academic community of study and support to doubts [82]. All processing was performed on a microcomputer with an Intel I-7 processor, with a processing speed of 2.8 GHz, RAM memory of 16 GBytes, HD capacity of 1 TByte, SSD 224 GBytes and Windows 10 operating system.

### 3.2 Methodological Approach

The methodological procedure was divided into three stages, as shown in the Fig. 4.

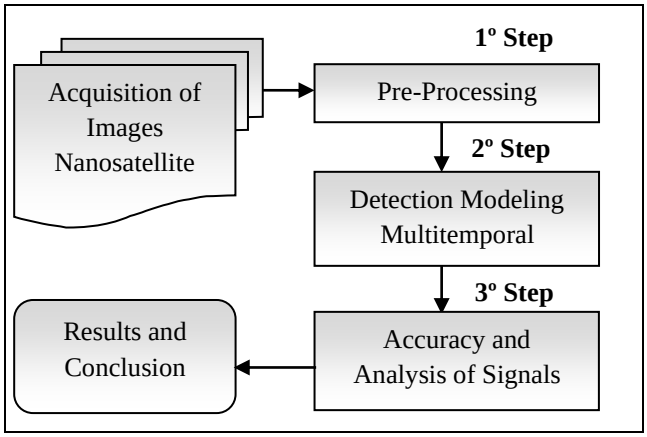


*Fig. 4: Macro flowchart of Methodology.*

### 3.2.1 Methodology – 1º Step

In the 1st stage, pre-processing of the images was carried out in order to allow the detection of seasonal bitemporal variation in the scenes. Thus, the selection and cuts of the study area were carried out, as well as the necessary treatments in the scenes for the complete effectiveness of the proposed methods. Thus, in the clippings, masks were created to delimit only the field of interest, in addition to converting the scenes to 8 bits. After several tests, it was decided to convert the images in order to improve performance and optimize the processing time when executing the models to detect anomalies.

### 3.2.2 Methodology – 2º Step

In the stage, a Multitemporal Detection Modeling was developed, where the method proposed in Python was implemented with the automated monitoring models Delta NDVI and Delta NIR. The stage aims to quantify the regions with positive, negative and between anomalies, in order to support the seasonal variations for decision making. Thus, according to the analyzed statistical criteria, an alert of message (signal) should be issued to signal possible loss of vegetation in the seasonal difference of the scenes, from pre-planting to harvest, going through the different stages of cultivation during the development of the culture, involving the entire production cycle.

In the Fig. 5 shows the macro task flowchart of the proposed and developed Anomalies models.

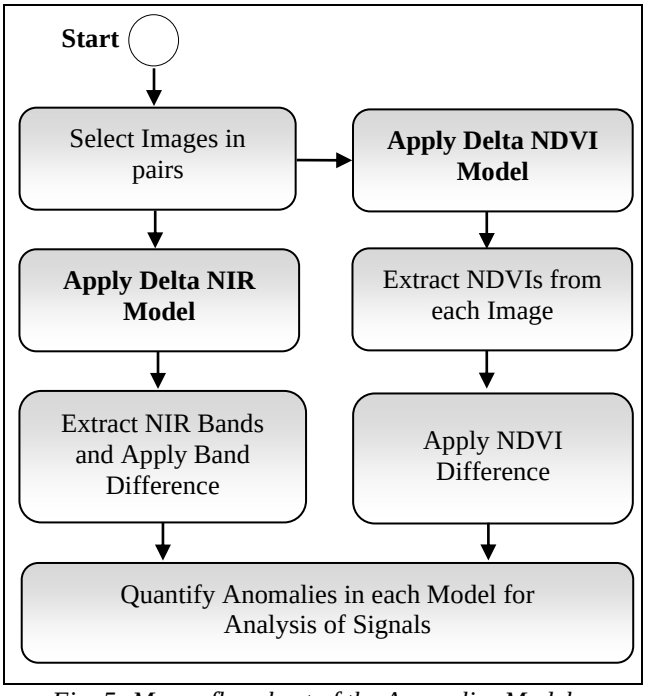


*Fig. 5: Macro flowchart of the Anomalies Models.*

For both models, the issuance of change detection warning signals will be carried out by measuring the tolerable loss of vegetation index, that is, the amount of negative anomalies in the difference image. Thus, the user will be able to customize in the tool a maximum acceptable range of vegetation loss for the monitored images. For each of the models, if the difference image shows a number of pixels for negative anomalies that is higher than the acceptable threshold of vegetative evolution defined by the user, the alert of message will be issued.

#### 3.2.2.1 Delta NDVI Model

In the Delta NDVI model, after selecting the pair of images to analyze the temporal change detections, the NDVI of each scene will initially be extracted, according to Equation 1. The vegetation index is generated from the loading of the metadata containing the band correction coefficients, in order to optimize the NDVI generation with a more assertive extraction. Then, the seasonal difference of NDVIs will be applied, where the mathematical operation of subtraction pixel by pixel between the most recent and the oldest scene will be performed, according to Equation 2.

In the generated Delta NDVI map, the greater the positive value of the analyzed areas, the greater the NDVI gain. However, the greater the negative value of the regions, the greater the loss of NDVI from the monitored areas. The regions with difference values close to zero correspond to the areas without significant changes, that is, with behavior according to the pattern they had been having [49].

If in the generated difference map there is a percentage of anomalies in the monitored areas, with a value higher than the defined acceptable% of changes, an alert will be issued in the model. In the histogram of the difference image of NDVIs, the range from $\mu$-1$\sigma$ to $\mu$ + 1$\sigma$ will contain pixels without significant occurrences of changes, according to the established standard deviation threshold ($\pm$ 1$\sigma$). Out of the range, at the ends of the histogram, are the pixels with significant changes during the temporal evolution between the images, being classified as negative and positive anomalies.

Negative anomalies are areas with probable loss of vegetation, with dark shades in the difference image, close to the nuances of black, indicating that in the older scene there was a higher positive NDVI index, compared to the most recent image. Thus, in the subtraction of NDVIs, the areas present low values, indicating the presence of vegetation in the oldest scene. Positive anomalies, on the other hand, are areas with a probable incidence of vegetation, being regions that present clear tones in the difference image, close to the white tint, indicating that in the oldest image there was a lower NDVI index, compared

to the most recent one. Therefore, when subtracting the NDVIs, the areas present high values, suggesting the presence of vegetation in the most recent scene compared to the oldest. As an example, they can be characterized as areas of regeneration of vegetation cover or cycles of agricultural practices. The regions between the anomalies, on the other hand, are areas without the significant presence of changes, that is, which maintained the behavior they had already been having according to the σ defined, presenting gray tones, oscillating between black and white [31].

In order to follow the vegetative cycle of crop development, in Table 2 are the expected values for healthy (in full force) and dry vegetation, as explained in the Fig. 1, in addition to the reflectance in the NIR and Red bands.

*Table. 2: Expected Values of Reflectances in the Vegetation Stages (HV: Healthy Vegetation, SV: Stressed Vegetation e DV: Dry Vegetation).*

| | HV | SV | DV |
|---|---|---|---|
| **NDVI** | 0.72 | 0.43, oscillating: 0.72 < Stressed < 0.14 | 0.14 |
| **NIR** | 50% | 45%, oscillating: 50% < Stressed < 40% | 40% |
| **RED** | 8% | 19%, oscillating: 8% < Stressed < 30% | 30% |

From the values listed for healthy and dry vegetation, as shown in the Fig. 1, the average intermediate estimates between the two vegetation extremes were derived, in order to characterize estimates for stressed vegetation. While a healthy vegetation, in the full cycle, has an expected NDVI value close to 0.72, a dry vegetation has a value around 0.14. Thus, based on the extreme values of healthy and dry vegetation, for an intermediate vegetation - in this case the stressed one between the two types - the average value of NDVI between the vegetations will be used. Thus, a stressed vegetation would probably have an average value close to 0.43, with average reflectance around 45% in the NIR and 19% in the Red Band. Therefore, it becomes possible to monitor the oscillation of vegetation quality through the values presented, performing a temporal monitoring in the vegetation growth cycle. While a crop has its maximum NDVI in the full cycle, in the initial cycle the value is minimal and is increased until the full cycle, after which it begins to regress, returning to the initial levels.

In the Fig. 6 shows the NDVI ranges for each type of vegetation, as shown in Table 2, making it possible, in addition to detecting anomalies, to verify the trend in vegetation quality based on the values indicated in the literature.

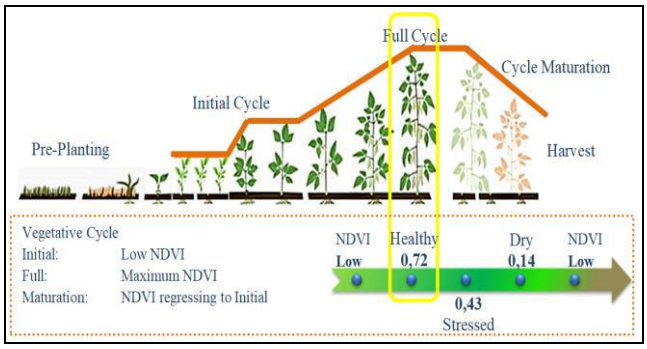


*Fig. 6: Vegetation Cycle with values adopted.*

### 3.2.2.2 Delta NIR Model

In the Delta NIR model, after selecting the pair of images for analysis of the temporal change detections, the NIR band will be extracted from each of the scenes, being band 4 of the Planet image. Then, the seasonal difference will be applied in the NIR bands, where the mathematical operation of subtraction pixel by pixel between the most recent and the oldest scene will be performed, according to Equation 3.

In the mathematical procedure performed, the subtraction represents a linear operation, in which the results will produce intensities outside the range of 0 to 255 pixels, requiring a contrast adjustment in order to avoid distortions in the statistical treatment when analyzing anomalies between the images. Thus, the range that represents the calculation of the operation, will be within the range of -255 to +255. In the implemented adjustment, the value of a constant of 255 will be added to the result, thus producing a new range from 0 to 510, and later, the range will be divided by 2, where the final range will be from 0 to 255, assuming a variation 256 shades of gray. Thus, when subtracting bands, values close to the mean of the difference interval will indicate regions of no change [18].

Similar to the Delta NDVI model, on the Delta NIR map generated from the difference in bands, in histogram around the average the pixels will be located without occurrences of changes. At the ends of the histograms, the pixels that had significant changes during the temporal evolution of the images will be concentrated. Thus, the generated subtraction image will be classified according to the standard deviation (σ) around the mean (μ), where the thresholds will be {[0, μ-σ [, [μ-σ, μ + σ],] μ + σ, 255]}. Thus, the values of (0 to μ-σ) are areas of negative

anomalies, with probable loss of vegetation, crop cutting or deforestation, of (μ-σ to μ + σ) are areas between anomalies, that is, without the significant presence of changes and (μ + σ up to 255) are areas of positive anomalies with probable areas of regeneration of vegetation cover [31].

The total number of pixels of the likely classes of changes will be compared with the acceptable threshold of changes defined, in order to detect anomalies. If the model detects changes in the monitored areas with a value greater than the acceptable% of changes stipulated, an alert will be issued in the model as a strong indication that there have been changes between the scenes.

### 3.2.3 Methodology – 3º Step

In the 3rd stage, the accuracy validation of the anomaly classifications and the analysis of Alerts signaling emissions were performed.

The anomalies classifications, obtained by the Delta NDVI and Delta NIR models, will be validated by means of a reference image. Such an image will be constructed through a visual classification by means of digitalization of the difference image of the scenes on screen, where each monitored scene will have the vectorized matrix representation. Therefore, the construction of the reference image aims to characterize the classes of positive, negative anomalies and regions between anomalies, according to the detection of light nuances close to the white tone (positive anomaly), dark ones close to black (negative anomaly) and oscillating in the gray tone (regions between anomalies without significant changes in temporal evolution). With the generation of each reference classification, the accuracy of the classifications pertinent to each model will be evaluated. The result of the classifications will be validated through a confusion matrix, where the accuracy of the classifications obtained by the implemented method will be verified. Thus, agreement and disagreement indices will be extracted - global accuracy, producer accuracy / omission errors, user accuracy / inclusion errors, Kappa and Tau indices, in addition to quantity and allocation disagreements - to validate the correct classified pixels or incorrectly in the model ratings. In addition, hypothesis Z tests will be applied in order to validate the null hypothesis of equality of the coefficients of agreement of the classifications.

The analysis of the signals will be performed by visual interpretation of the input images. The results will be compared in order to verify whether the signs should actually be emitted visually and / or if in the evaluation areas there were signs of some undetected signaling, in order to avoid false positives and / or negatives of detecting changes. Thus, the agricultural areas of the multitemporal application will be analyzed individually, being evaluated by means of interpretation keys as to color, shape and texture [34].

## IV. RESULTS AND DISCUSSIONS

The Fig. 7 shows the monitoring for the vegetative cycle of the stand from the initial, full, maturation to cut for the Delta NDVI Model. For each image comparison, the difference NDVI image was extracted (both in gray level and in colored composition, in order to facilitate visual interpretation), the percentage of anomalies resulting from the difference image, as well as the analysis of the vegetative cycle for the crop with vegetation quality indicators in the healthy, stressed and dry categories, according to the premises adopted and provided in Table 2.

Delta NDVI's developed method takes an average of 25 seconds to process areas up to 100 ha. The oscillation values around the mean were tested with standard deviation of 1 and 2, where it was detected that for the value of 2σ practically 100% of the pixels were labeled as areas without the presence of anomalies. Thus, in order to be as sensitive as possible to signaling the change detections, in addition to providing for the use of smaller plots (which encompass most rural properties in the country), where the use of a larger standard deviation could not detect changes, we chose to use 1σ for the Delta NDVI and Delta NIR models.

As can be seen in the Fig. 7, in the NDVI images difference for vegetative cycles 1 to 8, the areas where in the color difference image, have nuances of medium to darker green, according to the color legend with the scale in the figure, are regions with vegetation incidence in the most recent image compared to the oldest, being classified as positive anomalies. Still, in the NDVIs images, difference between the scenes, in the gray level image, the anomalies have nuances close to the white tint, as can be seen.

Negative anomalies are areas in which the color difference image has shades of medium to darker red, according to the color scale in the figure. In the NDVIs images, the difference between the scenes, in the gray level image, the anomalies have dark nuances close to the black tint. The areas between anomalies, in the color difference image, have colors ranging from light red, through yellow to light green. In NDVI images, difference between the scenes, in gray images the anomalies have nuances close to the gray tone, oscillating between black and white. Thus, it is possible to observe in which regions of the field the NDVI value decreased in relation to the analyzed period and in which it increased, being an indication of growth or loss of vegetation in the crop.

For all simulations, a tolerable percentage of up to 1% of vegetation loss was established, that is, of a negative anomaly, aiming to capture any change that occurred between the scenes. Thus, as the number of negative anomalies was higher than the percentage established in all images, differences from Cycles 1 to 8, due to the standard deviation applied, automated warning signals were issued for all classifications. Also, according to Fig. 7, in all classifications the percentage of regions without significant changes was greater than 50%.

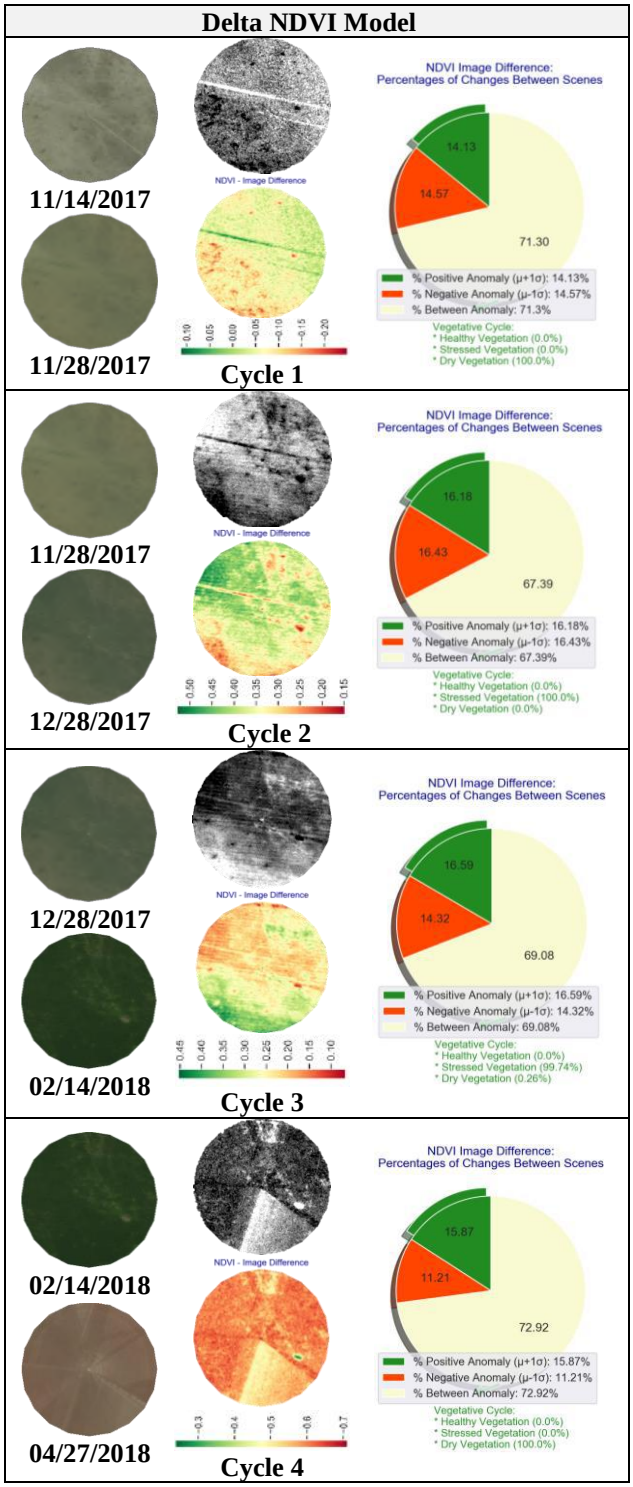


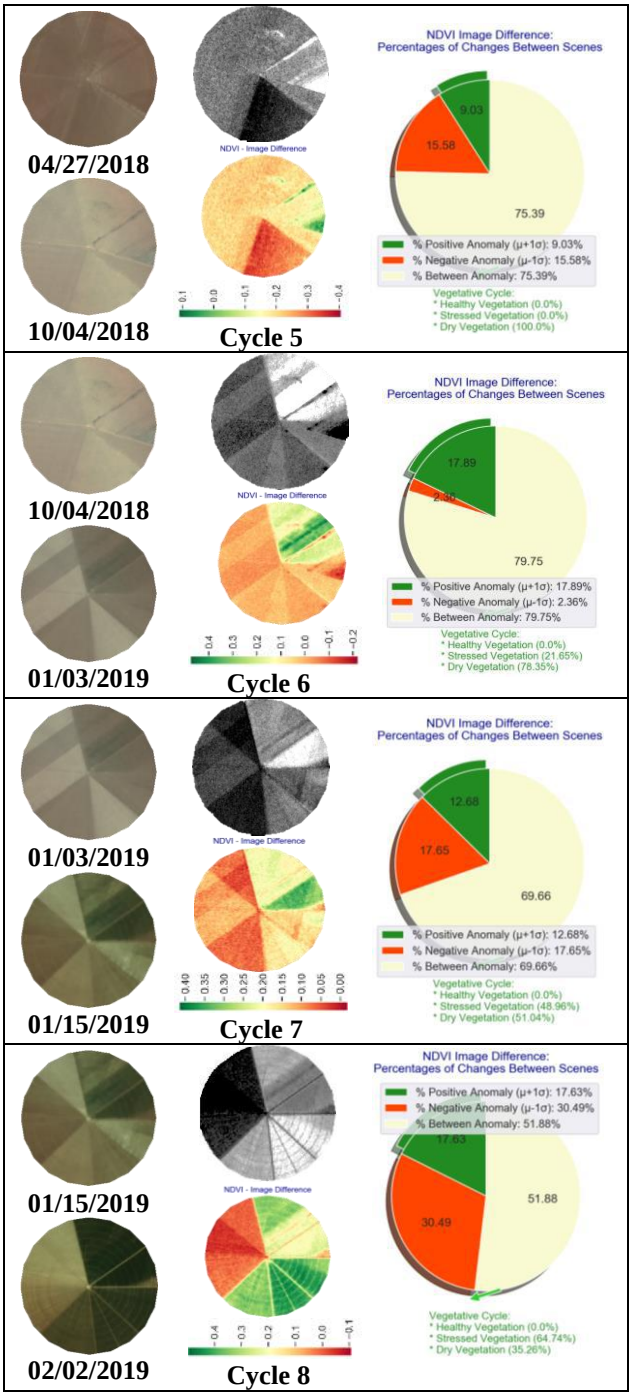


*Fig. 7: Delta NDVI Model with Vegetative Cycle, from initial, full, maturation and cutting.*

Through the vegetative cycle, it was possible to capture the vegetational quality between the scenes, where from the difference image of NDVIs it was found that the vegetations were found largely in the vegetative cycle of dry and stressed foliage, the latter being a classification intermediate between healthy and dry state. Still, according to the scale with the NDVI values of the scenes, the lower values represent absence of vegetation, thus being in the initial vegetative cycle, and the maximum values are an indication that the crop has reached its full

stage of development, where the process begins maturation in which the levels begin to regress until the harvest, when the preparations for the beginning of a new cycle begin. As can be seen in Cycle 1, the maximum NDVI value of the difference image is around 0.10, indicating low presence of vegetation in the scene and an exposed soil that may be being prepared for planting. In Cycle 2, with imaging one month after Cycle 1, with an image difference between the scenes of 11/28/2017 and 12/28/2017, the maximum value becomes 0.50, thus indicating a planting in development of the crop with stressed vegetation, using the parameters shown in the Fig. 6, towards the full vegetation stage. In Cycle 3, with a difference image with an image of two months after the previous cycle, the maximum value becomes 0.45, indicating a probable achievement of the full stage during the period and decreasing the values in the possible stage of crop maturation. In Cycle 4, the maximum value becomes 0.30 indicating probable harvest and soil being prepared for planting, in line with the elucidated in Cycle 5 with a maximum value of 0.10, as interpreted in the scenes in the Fig. 7. In Cycles 6, 7 and 8 there are indications of the different nuances of vegetation and exposed soil, with maximum values of 0.40 indicating the development process of horticultural farming practices in the stand.

Through the automated extraction of anomalies, as in the Fig. 7, for different types of crop development, it was possible to monitor changes and monitor the development cycle, sending signals of either loss of vegetation or forest degradation based on the percentage of negative anomalies, regarding the monitoring of vegetation growth or areas of regeneration of vegetation cover and cycles of agricultural practices, through the percentage of positive anomalies, in addition to the predominance of foliage in the vegetative cycle. In the images of Cycle 5, although both Planet scenes indicate the presence of exposed soil, the most recent image appears lighter nuances and closer to white indicating less remnants of vegetation in the comparison between the scenes. Thus, one of the possible causes may be the soil being prepared for planting with products in the soil.

In the Fig. 8 shows the monitoring for the vegetative cycle of the stand from the initial, full, maturation to cut for the Delta NIR model. For each image comparison, the difference scenes of NIR bands were extracted (both in gray level and in colored composition, in order to facilitate visual interpretation). Also, similarly to the Delta NDVI Model, the percentages of anomalies resulting from the difference image were extracted.

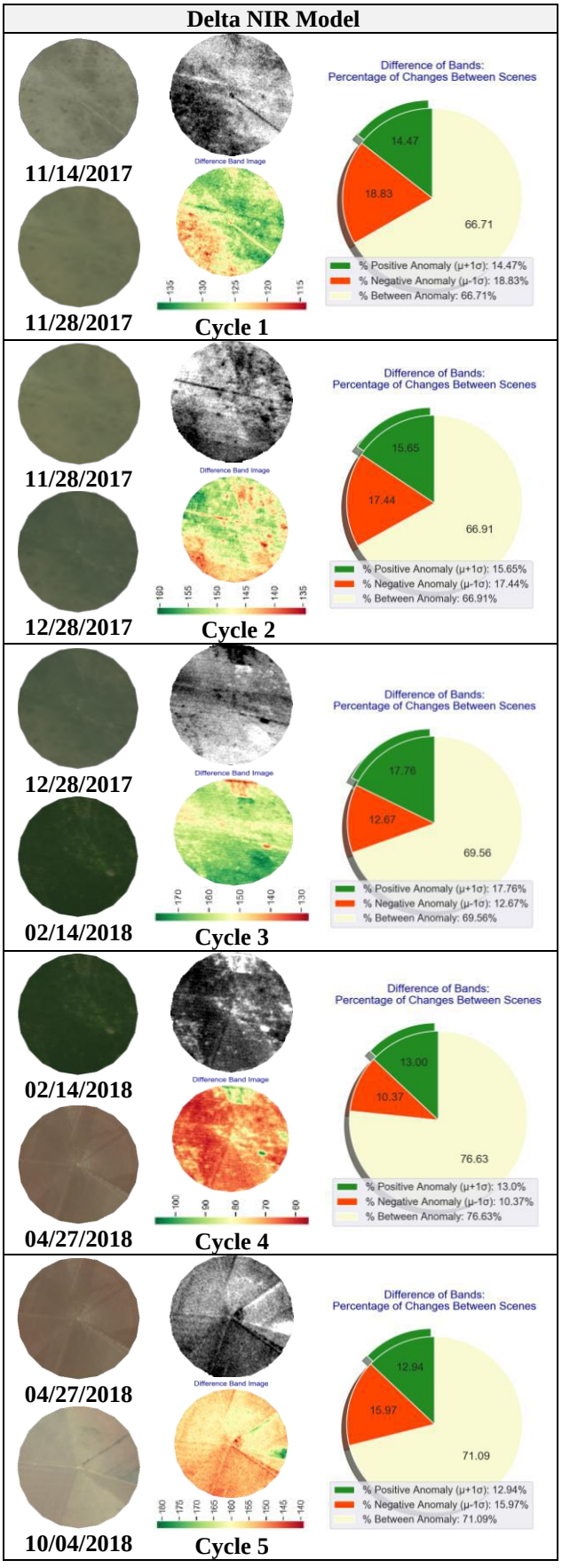

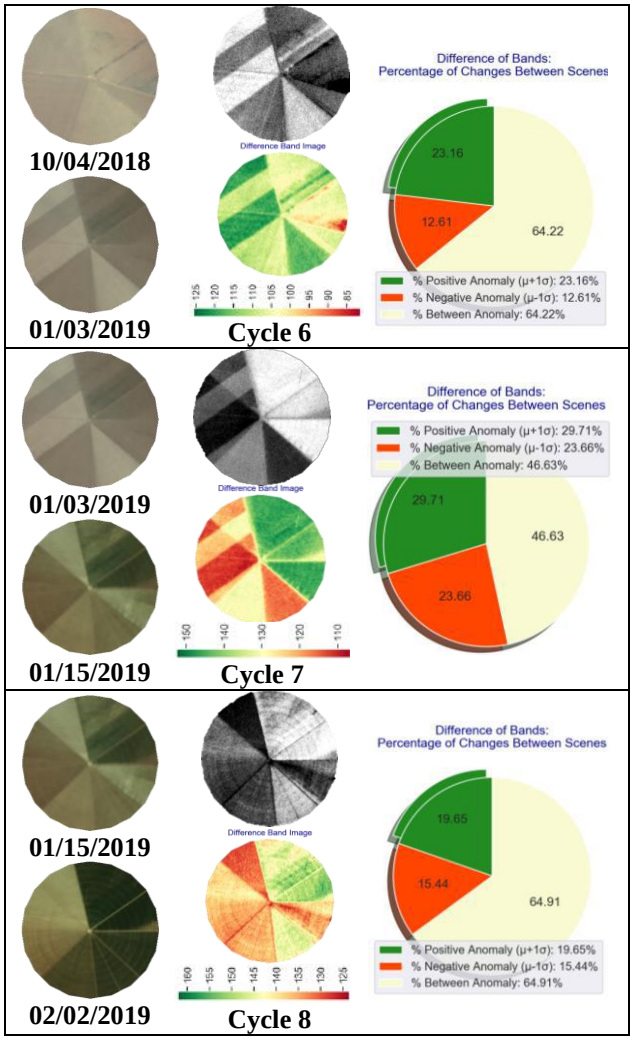


*Fig. 8: Delta NIR Model with Vegetative Cycle, from initial, full, maturation and cutting.*

The implemented Delta NIR method takes an average of 11 seconds to process areas up to 100 ha. Therefore, in terms of performance, the processing time is less than half that performed for the Delta NDVI model. When it comes to a few areas, seconds can be irrelevant. However, in the monitoring schedule for a significant volume of areas, the response time becomes relevant for eventual inspection of the areas and decision making.

As can be seen, in the NIR images difference for vegetative cycles 1 to 8, the areas in which in the color image, have nuances of medium to dark green, according to the color legend with the scale in the figure, are regions with vegetation incidence in the most recent image compared to the oldest, being classified as positive anomalies. Also, in the NIR images the difference between the scenes, in the gray level image, the anomalies have nuances close to the white tint, as can be seen in the figure.

Negative anomalies are areas in which the color difference image has shades of medium to darker red, according to the color scale in the figure. In the NIR images, difference between the scenes, in the gray level image, the anomalies have dark nuances close to the black tint. The areas between anomalies, in the color difference image, have colors ranging from light red, through yellow to light green. In NIR images, difference between scenes, in gray level images, anomalies have nuances close to the gray tonality, oscillating between black and white. Thus, analyzing the difference in NIR bands, it is possible to observe in which regions of the field the value of NIR decreased in relation to the analyzed period and in which it increased, being an indicator of the quality and incidence of the culture, where according to Table 2 a healthy vegetation has higher levels of reflectance in the NIR (50%) compared to dry vegetation (40%) or even absence of vegetation.

In order to establish comparisons with the Delta NDVI model, in the same way as for the model, for all simulations, a tolerable percentage of up to 1% of vegetation loss was established, that is, of negative anomaly, aiming to capture any change that occurred between the scenes. Thus, as the number of negative anomalies was higher than the established percentage of 1% in all images, differences from Cycles 1 to 8, due to the standard deviation applied, automated warning signaling was issued for all classifications.

In comparing the difference images for each of the cycles of Fig. 7 and Fig. 8, considering the model Delta NDVI and Delta NIR, it was observed that when there is greater homogeneity in the plots, as it happens for Cycles 1 to 5, for regions without significant changes in changes (between anomalies), the comparative variation between models was less than 10%. Thus, it is concluded that both models similarly detected the number of regions without changes in the temporal variation, as shown in Table 3.

It is important to inform that when there is a greater diversity of cultures in the field, according to the difference in Cycles 6 to 8 of Fig. 7 and Fig. 8, the variation between the models was greater than 10% for regions between anomalies. Thus, a possible cause for the variation was due to the influence of the red band of the visible complemented to the near infrared in the Delta NDVI model, which were more sensitive to the radiometric variation of the study target in the time comparison, being that the Delta NIR model considered only the near infrared band.

For the detection of positive and negative anomalies, the percentage variation between models was also smaller for polygons with greater homogeneity. The greatest variation occurred in the difference image of Cycles 6 and 8, as shown Fig. 7 e Fig. 8. For Cycle 6 Delta NDVI

detected a negative anomaly of 2.36% and a positive one of 17.89%, whereas for Delta NIR the anomalies were respectively 12.61 % and 23.16%. For Cycle 8, Delta NDVI detected a negative anomaly of 30.49% and a positive one of 17.63%, while for Delta NIR the anomalies were 15.44% and 19.65%, respectively. Thus, the greater variation between models for plots with greater crop heterogeneity, indicate that the distinct nuances within the plot produced more sensitive spectral responses when aggregating the red band information of the Delta NDVI model, compared to the Delta NIR model.

*Table. 3: Variation of Anomalies in the Models.*

| | **Anomalies: Variation (Δ) of Models Delta NDVI x Delta NIR** | | |
|---|---|---|---|
| | **Δ Between Anomaly** | **Δ Negative Anomaly** | **Δ Positive Anomaly** |
| **Cycle 1** | -6.88% | 24.96% | 2.35% |
| **Cycle 2** | -0.72% | 5.79% | -3.39% |
| **Cycle 3** | 0.69% | -13.02% | 6.59% |
| **Cycle 4** | 4.84% | -8.10% | -22.08% |
| **Cycle 5** | -6.05% | 2.44% | 30.22% |
| **Cycle 6** | -24.18% | 81.28% | 22.75% |
| **Cycle 7** | -49.39% | 25.40% | 57.32% |
| **Cycle 8** | 20.07% | -97.47% | 10.28% |
| **Mean** | **2.66%** | **13.01%** | **-7.70%** |
| **Median** | **4.12%** | **8.43%** | **-3.38%** |

Considering the average and median values of variation (Δ) between the models, as shown Table 3, for the eight development cycles of the field presented in the Fig. 7 and Fig. 8, in the areas without significant changes in the changes, the oscillation between the models was 2.66% on average and 4.12% in median. For the negative anomalies of the cycles, the values were an average of 13.01% and a median of 8.43%. As for positive anomalies, the variation between the models was on average -7.70% and -3.38% in median, thus showing little variation between the models.

With the extraction of the classifications of the Delta NDVI and Delta NIR models, the accuracy of the anomaly classifications was verified, according to the results presented in the Fig. 9. The validation of the classifications was performed with the reference image obtained by vectorization by visual interpretation, where studies show that when the visual classification is used as a reference map of the real scenario, it allows the reduction of the classification error with a consequent increase in global accuracy [70] [83].

In the Fig. 9 shows, for each of the eight vegetative monitoring cycles of the field, the anomalies classifications extracted for the Delta NDVI and Delta NIR models, in addition to the reference image used in the validation of the classification of each cycle. In red color are the regions of negative anomalies, in green are the regions of positive anomalies and in blue color are the regions between anomalies.

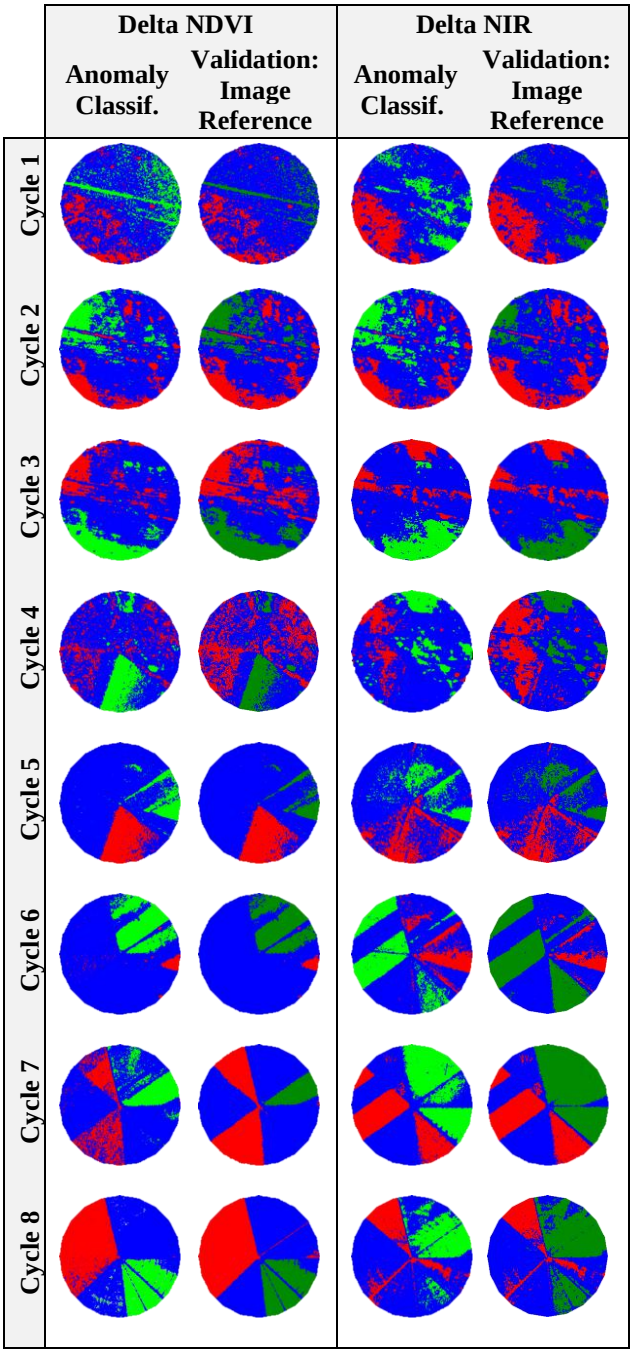


*Fig. 9: Anomalies Classifications with the respective reference images for Validation of Accuracies.*

When comparing Fig. 7 and Fig. 8 with the Fig. 9, it can be seen that the light nuances, close to the white hue in the image resulting from the difference between the scenes, indicate growth of the vegetation being classified in the green hue. The darker areas, close to black, indicate loss of vegetation in the image resulting from the difference between the scenes, being classified in red. The regions oscillating in gray, are regions that did not have significant changes in the temporal evolution between the images, being classified in blue color.

For all bitemporal classifications performed, the accuracy metrics were extracted, as shown in Table 4. Therefore, the Global Accuracy (G.A.), Kappa (K), Tau (T) and Global Disagreement measures were generated of the classifications, being obtained by the sum of the Quantity Disagreement (Q.D.) and the Allocation Disagreement (A.D.). To test the statistical significance between the Kappa indices, 95% confidence intervals for the coefficient were constructed for each classification, where bilateral Z hypothesis tests were performed in order to verify possible equalities between the classifications at the 5% significance level. Thus, the null hypothesis was tested in order to analyze whether it would be accepted or rejected based on the comparison of the p-value with the adopted significance level, where considering the tabulated Z value of 1.96 for the 5% significance level, the results of classifications with Z tests greater than 1.96 or less than -1.96 would be considered statistically different. Therefore, for classifications with Z calculated between -1.96 and 1.96, the hypotheses of equality between the classifications would be accepted.

Analyzing the information, especially in the Z test, it became evident that the confusion matrices of the Delta NDVI model classifications are different from the Delta NIR model classifications, considering the same parameters of the classifications and study regions. Although the premise of the models is similar for the detection by anomaly classification, whether for positive, negative anomalies and regions between anomalies through the use of ratio and difference of bands between the images, it was possible to infer that at the 5% significance level none of the confusion matrices of the classifications is statistically equal, based on the calculated Z value and the p-value. Also, considering the calculated Z, the p-value for the classifications was less than 0.002, less than the 5% significance level, the result being statistically significant and rejecting the null hypothesis of equality between the classifications.

Considering the mean and median values of the indices presented in Table 4, the greatest global accuracy was obtained in median and when the Delta NDVI model was used, obtaining a G.A. of 92.31%. Thus, the Delta NDVI model presented results of classification of detection of higher changes in relation to the Delta NIR model, considering G.A., Kappa, Tau, in addition to a smaller global disagreement error considering the sum of the disagreements of quantity and allocation.

*Table. 4: Accuracies of Delta NDVI and Delta NIR Models for the Classifications.*

| Cycle | Delta NDVI (ND) x Delta NIR (NI) | | | | | | Z-Test $H_0: K_1 = K_2$ $H_1: K_1 \neq K_2$ | |
|---|---|---|---|---|---|---|---|---|
| | **ND NI** | **G.A. (%)** | **K** | **T** | **Q.D. (%)** | **A.D. (%)** | **Z Score** | **95% Conf** |
| **1** | ND | 92.59 | 0.83 | 0.89 | 7.4 | 0.0 | -28.04 | ≠ |
| | NI | 95.73 | 0.91 | 0.94 | 4.3 | 0.0 | | |
| **2** | ND | 92.03 | 0.85 | 0.88 | 8.0 | 0.0 | 37.19 | ≠ |
| | NI | 86.25 | 0.73 | 0.79 | 7.7 | 6.0 | | |
| **3** | ND | 84.92 | 0.72 | 0.77 | 15.1 | 0.0 | -72.92 | ≠ |
| | NI | 96.72 | 0.93 | 0.95 | 1.6 | 1.6 | | |
| **4** | ND | 82.65 | 0.67 | 0.74 | 15.0 | 2.3 | -18.75 | ≠ |
| | NI | 88.01 | 0.74 | 0.82 | 12.0 | 0.0 | | |
| **5** | ND | 97.00 | 0.92 | 0.95 | 2.1 | 0.9 | -43.87 | ≠ |
| | NI | 100 | 1.0 | 1.0 | 0.0 | 0.0 | | |
| **6** | ND | 97.93 | 0.94 | 0.97 | 1.2 | 0.9 | 73.76 | ≠ |
| | NI | 85.11 | 0.72 | 0.78 | 9.6 | 5.3 | | |
| **7** | ND | 84.96 | 0.7 | 0.77 | 9.6 | 5.5 | -49.74 | ≠ |
| | NI | 90.38 | 0.85 | 0.86 | 9.6 | 0.0 | | |
| **8** | ND | 95.08 | 0.92 | 0.93 | 3.9 | 1.0 | 63.57 | ≠ |
| | NI | 85.86 | 0.75 | 0.79 | 12.1 | 2.0 | | |
| **Mean** | **ND** | **90.90** | **0.82** | **0.86** | **7.79** | **1.33** | G.D. 9.12% | |
| | **NI** | **91.01** | **0.83** | **0.87** | **7.11** | **1.86** | G.D. 8.97% | |
| **Median** | **ND** | **92.31** | **0.84** | **0.89** | **7.70** | **0.90** | G.D. 8.60% | |
| | **NI** | **89.20** | **0.80** | **0.84** | **8.65** | **0.80** | G.D. 9.45% | |

*ND: Delta NDVI; NI: Delta NIR; G.A.: Global Accuracy; K: Kappa Coefficient; T: Tau; Q.D.: Quantity Disagreement; A.D.: Allocation Disagreement; G.D.: Global Disagreement; 95% Conf: 95% Confidence; ≠: Classifications are Differents; =: Classifications are Iguals.

With the results of the classifications there were variations between the different agricultural practices present in the short and annual cycle plot in terms of accuracy where in general more homogeneous areas with less transformation in the time of the crop development cycle had significant assertiveness as in Cycle 5 with exposed soil transitions with 97% G.A. for Delta NDVI and 100% for Delta NIR. Still according to the results of the classifications the more heterogeneous the crops within the field that is the diversity of cultures there is a tendency of less being the global accuracy and agreement indexes in comparison to the cultures in the field with homogeneous areas as in Cycle 7 with 84.96% G.A. for Delta NDVI and a Kappa of 0.7 and Tau of 0.77.

In Cycle 4 the difference image of the NDVI model showed the lowest G.A. among the classifications with 82.65% for a Kappa of 0.67 and Tau of 0.74. Although it appears to have low diversity in the field visually and there are characteristics of transition from vegetation to exposed soil different nuances are observed in the field due to the color transition in the gray level. Thus, it is likely that the extracted accuracy was impacted by mixtures within the plot such as soil being prepared for planting.

Although the Delta NDVI model has obtained superior results in relation to the Delta NIR, according to a median of 92.31% for the eight cycles, the Table 5 it can be observed that there were few variations in the accuracy in the general comparison of the mean and median values for the classifications extracted from both models.

Considering the average values of the classifications Delta NIR presented results slightly superior to the Delta NDVI Model, with G.A. of 91.01% versus 90.90%, according to the Table 5. Thus, the Delta NDVI classifications had an overall accuracy variation of 0.12% lower while for the Kappa and Tau indices the oscillation was around 1% lower.

However, the median as it is a measure of central tendency and less sensitive to outliers compared to the average can represent in a more assertive way the real general result of the classifications. Even so although Delta NDVI showed higher values compared to Delta NIR the variation was low.

For overall accuracy Delta NDVI ratings were 3.49% higher while Kappa was 5% higher. Considering the global disagreement, the variation was around 9% when comparing the models.

*Table. 5: Comparisons of mean and median values for the Delta Models Classifications.*

| | | Delta NIR | Delta NDVI | ΔNDVI x ΔNIR |
|---|---|---|---|---|
| **Mean** | **G.A. (%)** | **91.01** | 90.90 | -0.12% |
| | ***Kappa*** | **0.83** | 0.82 | -1.20% |
| | ***Tau*** | **0.87** | 0.86 | -1.15% |
| | **Q.D. (%)** | **7.11** | 7.79 | 9.56 |
| | **A.D. (%)** | **1.86** | 1.33 | -28.49% |
| **Median** | **G.A. (%)** | 89.20 | **92.31** | 3.49% |
| | ***Kappa*** | 0.80 | **0.84** | 5% |
| | ***Tau*** | 0.84 | **0.89** | 5.95% |
| | **Q.D. (%)** | 8.65 | **7.70** | -10.98% |
| | **A.D. (%)** | 0.80 | **0.90** | 12.5% |

**ΔNDVI x ΔNIR:** Variations between Delta NDVI and Delta NIR Models.

In the Fig. 10 show the 95% confidence intervals (I.C.) for each of the Kappa coefficients obtained for the classifications performed. The I.C. takes into account the standard error which is obtained by dividing the standard deviation by the square root of the sample size. The classification with maximum Kappa value was obtained for Cycle 5 in the difference image of bands with Delta NIR where the confidence interval had a value of 0.98 at the lower limit demonstrating the excellence of the classification at the level of significance adopted.

The lowest Kappa index was for Cycle 4 in the difference image with the Delta NDVI with a value of 0.67. With the 95% confidence interval, the range of value for that classification ranged from 0.65 to 0.69. By visual inspection of the scene in the Fig. 8 and Fig. 9, although initially it appears to have low diversity in the plot and there are characteristics of transition from vegetation in the image from 02/14/2018 to soil exposed in the image from 04/27/2018, it is observed Fig. 9 shows that due to the reference image used in the validation the greatest confusion was due to classes that should be classified as negative anomaly with loss of vegetation (red color) and were classified by the model as regions between anomalies that is without significant changes the temporal evolution (blue color). Thus, it is likely that the extracted accuracy

was impacted by mixtures within the plot such as soil being prepared for planting which made it not so homogeneous in the transition period between scenes.

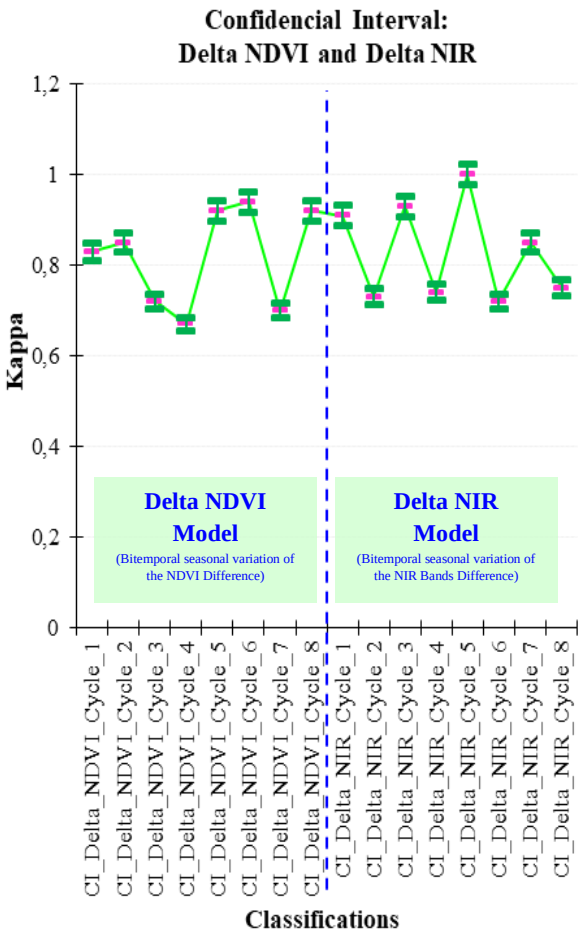


*CI_Delta_NDVI (Classification Confidence Interval for Anomalies of the Delta NDVI Model)ç
*CI_Delta_NIR (Classification Confidence Interval for Anomalies of the Delta NIR Model).

*Fig. 10: Confidence Interval: Comparative of the Delta Models.*

## V. CONCLUSION

The application of tool developed in Python, called LimiariZC, with the development of modules for Delta NDVI and Delta NIR models, allowed the percentage of positive negative anomalies and areas without significant changes to be quantified by seasonal differences in addition to metrics of the vegetative cycle of the crop (indicating the percentage of healthy stressed and drought) presenting what actually happened in the field and aggregating information for decision making, by those responsible for the release of agricultural financings.

Although the proposed models of Delta NDVI and Delta NIR have the same assumptions and guidelines for detecting anomalies through the image resulting from the bitemporal seasonal difference between the scenes it was found that the classifications are statistically different when compared to each other being that the statistical tests applied showed that the models are different. In addition, the seasonal difference applied to the images causes and brings the normalization of the data. Therefore, it provides for possible atmospheric attenuations with the models benefiting from normalization.

The results obtained in the anomaly classifications indicate that the Delta NDVI model presented slightly superior results in relation to the Delta NIR. In this way the probable potentiation of the ratio between bands when NDVI extraction (which highlights the vegetation making it expressive in the scene) preceding the delta difference between the images makes it possible for the classifications to be more assertive on average.

However, it should be noted that the variation was not significant in addition to the fact that on average the Delta NIR classifications obtained superior results which leads to the conclusion that depending on the desired purpose the Delta NIR applicability is an attractive alternative for detecting changes. Due to the model using only one band in the detection it makes the processing less costly with lower cost with low processing time and good performance and the tests indicated that the method was executed in less than half of the model execution time Delta NDVI.

The results obtained from anomaly detection both in the Delta NDVI model and in the Delta NIR model, showed that the models can be used as a significant indicator of oscillation and multitemporal trends in land use and cover. Still, it was found that the percentage values of anomalies and regions without significant changes are strongly correlated to the dispersion value around the adopted average that is the standard deviation around the average. Thus, it is concluded that the lower the standard deviation value the higher the percentages of positive and negative anomalies the smaller the region with areas of non-changes. Therefore, for the sensitivity of the models in order to emit conservative signals the lower the standard deviation value adopted the greater the detection of the quantity of anomalies and consequently more easily signals of changes in the vegetation cover will be triggered.

In addition, the low response time in processing (around 25 seconds for Delta NDVI and 11 seconds for Delta NIR) for executing of the models on the tool developed, when use areas of up to 100 ha (which represent almost 90% of the rural properties from country

used as test), add reduced operating and investment cost by not requiring on-site inspection, add innovation and differential making the proposed models effective and attractive for detecting changes without necessarily carrying out on-site visits and in line with the Government Consultancy for agricultural financings with the recommendation of Central Bank of Brazil and and which can be extended to other countries due to population growth and the need for new areas for planting with the consequent release of agricultural credits. Thus, the methodology aims to monitor the development of cultures, reducing face-to-face work.

Finally, although the models were applied in a study area in Brazil, can be used in any region of the planet for monitoring areas with agricultural financings or that will be financed, allowing greater control and inspection by those responsible for releasing agricultural credit, that usually has government subsidies.

## REFERENCES


[1] Alexandratos, N., Bruinsma, J. (2012). World agriculture towards 2030/2050: the 2012 revision.

[2] Aune-Lundberg, L., Stand, G. H. (2019). CORINE Land Cover.

[3] Azeredo, M., Monteiro, A. M. V., Escada, M. I. S., Ferreira, K. R., Vinhas, L., Pinheiro, T. F. (2016). "Mineração de trajetórias de mudança de cobertura da terra em estudos de degradação florestal". Revista Brasileira de Cartografia 68 (4): 717-731.

[4] BACEN, Banco Central do Brasil. (2015). Resolução nº 4.427. de 25 de Junho de 2015. Diário Oficial da República Federativa do Brasil.

[5] Bezerra, M. V. C., Silva, B. B., Bezerra, B. G. (2011). "Avaliação dos efeitos atmosféricos no albedo e NDVI obtidos com imagens de satellite". Revista Brasileira de Engenharia Agrícola e Ambiental 15 (7): 709-717. doi: 10.1590/S1415-43662011000700009.

[6] Bey, A., Sánchez-Paus Díaz, A., Maniatis, D., Marchi, G., Mollicone, D., Ricci, S., Patriarca, C. (2016). "Collect earth: Land use and land cover assessment through augmented visual interpretation". Remote Sensing 8 (10): 807. doi:10.3390/rs8100807.

[7] Bonato, M. (2009). Projeto Agrobrasília. Universidade de Brasília. Brasília.

[8] Brito, J. L. S., Prudente, T. D. (2005). "Mapeamento do uso da terra e cobertura vegetal no município de Uberlândia-MG utilizando imagens CCD/CBERS 2". Caminhos da Geografia 13:144-153.

[9] Câmara, G., Vinhas, L., Ferreira, K. R., De Queiroz, G. R., De Souza, R. C. M., Monteiro, A. M. V, De Freitas, U. M. (2008). "TerraLib: An open source GIS library for large-scale environmental and socio-economic applications". In: Open source approaches in spatial data handling. Springer. Berlin. Heidelberg. 247-270. doi: 10.1007/978-3-540-74831-1_12.

[10] CNA. Confederação da Agricultura e Pecuária do Brasil. (2020). PIB do Agronegócio. Brasília.

[11] Canty, M. J. (2019). Image analysis. classification and change detection in remote sensing: with algorithms for Python. CRC Press.

[12] Carvalho Junior, O. A., Hermuche, P. M., Guimarães, R. F. (2006). "Identificação regional da floresta estacional decidual na bacia do Rio Paraná a partir da análise multitemporal de imagens MODIS". Revista Brasileira de Geofísica 24 (3): 319-332.

[13] Cervantes-Godoy, D., Dewbre, J. (2010). Economic importance of agriculture for poverty reduction. "Economic Importance of Agriculture for Poverty Reduction". doi: 10.1787/5kmmv9s20944-en

[14] César, P. G. B. (2019). "Detecção de mudanças de uso e cobertur da terra por imagens de nanossatélites: estudo de caso do entorno da Aldeia Verdadeira (Anhetenguá)". Dissertação de Mestrado em Sensoriamento Remoto, Universidade Federal do Rio Grande do Sul.

[15] CONAB, Companhia Nacional de Abastecimento. (2016). Acompanhamento da Safra Brasileira. Grãos. Safra 2016/17. Observatório Agrícola. 4:164.

[16] CONAB, Companhia Nacional de Abastecimento. (2019). Acompanhamento da Safra Brasileira. Grãos. Safra 2018/19. Observatório Agrícola. 12: 47.

[17] Coppin, P., Jonckheere, I., Nackaerts, K., Muys, B., Lambin, E. (2004). "Digital Change Detection Methods in Ecosystem Monitoring: A review". International Journal of Remote Sensing 9:1565-1596. doi: 10.1080/0143116031000101675.

[18] Crosta, A. P. (2002). Processamento Digital de Imagens de Sensoriamento Remoto. UNICAMP.

[19] De Lima, M. I. C. (2009). Projeto Radam: Uma Saga na Amazônia. Paka-Tatu.

[20] De Oliveira, B. N., Filgueiras, R., Venancio, L. P., Mantovani, E. C. (2017). "Predição da produtividade de milho irrigado com auxílio de imagens de satélite". Revista Brasileira de Agricultura Irrigada 11 (4): 1627. doi: 10.7127/rbai.v11n400567.

[21] De Wit, A., Boogaard, H., Fumagalli, D., Janssen, S., Knapen, R., Van Kraalingen, D., Van Diepen, K. (2019). "25 years of the WOFOST cropping systems model". Agricultural Systems 168: 154-167. doi: 10.1016/j.agsy.2018.06.018.

[22] Della Justina, D. D., De Lima, P. H. P., De Sousa, C. H. W., Oldoni, L. V., Johann, J. A., Mercante, E. (2013). "Geração de perfis espectro-temporais de NDVI para diferentes cultivares de soja". In: XVI Simpósio Brasileiro de Sensoriamento Remoto. Foz do Iguaçu-PR, Brasil, 8838-8844, April 13-18.

[23] Dias, C. N., Jardim, F., Sakuda, L. O. (2019). Radar AgTech Brasil 2019: Mapeamento das Startups do Setor Agro Brasileiro. Embrapa. SP Ventures e Homo Ludens.

[24] Eastman, J. R., Mckendry, J. E., Fulk, M. A. (1995). Change and Time Series Analysis. UNITAR. Clark University. Worcester. USA.

[25] Ehlers, M., Sofina, N., Filippovska, Y., Kada, M. (2014). "Automated techniques for change detection using combined edge segment Texture Analysis, GIS and 3D

Information". In: Global urban monitoring and assessment through Earth observation. CRC Press. doi: 10.1201/b17012-22.

[26] EMBRAPA, Empresa Brasileira de Pesquisa Agropecuária. (2018). Agricultura Familiar Produção Vegetal. Embrapa.

[27] EMBRAPA, Empresa Brasileira de Pesquisa Agropecuária. (2021). Estudos socioeconômicos e ambientais. "O Agro no Brasil e no Mundo: Uma Síntese do Período de 2000 a 2020".

[28] FAO, Food and Agriculture Organization of the United Nations, International Fund for Agricultural Development, World Food Programme. (2015). The State of Food Insecurity in the World. Meeting the 2015 international hunger targets: Taking Stock of Uneven Progress.

[29] FAOSTAT, Food and Agriculture Organization of the United Nations. (2018). Major Commodities Exporters. Countries by Commodity. Rankings.

[30] Feranec, J., Soukup, T., Hazeu, G., Jaffrain, G. (2016). European landscape dynamics: CORINE land cover data. CRC Press.

[31] Ferrari, J. L., Santos, A. R., Garcia, R. F. (2011). "Análise da Vegetação por Meio da Subtração de Imagem NDVI na Sub-Bacia Hidrográfica do Córrego do Horizonte Alegre-ES". Engenharia Ambiental 8 (3): 3-18.

[32] Ferreira, L. G., Huete, A. R. (2004). "Assessing the seasonal dynamics of the Brazilian Cerrado vegetation through the use of spatial vegetation indices". International Journal and Remote Sensing 25 (10): 1837-1860. doi: 10.1080/0143116031000101530.

[33] FIESP, Federação das Indústrias do Estado de São Paulo. (2016). Informativo Deagro 2016. Safra Brasileira de Grãos 2016/2017. FIESP.

[34] Florenzano, T. G. (2011). Iniciação em Sensoriamento Remoto. Oficina de Texto.

[35] Gandhi, G., Parthiban, S., Nagaraj, T., Christy, A. (2015). "Ndvi: Vegetation change detection using remote sensing and gis - A case study of Vellore District.", Procedia Computer Science 57: 1199-1210. doi: 10.1016/j.procs.2015.07.415.

[36] Ghesti, L. V. (2009). Programa de assentamento dirigido do Distrito Federal – PAD/DF: Uma realidade que superou o sonho. Brasília.

[37] Godoy, C. V. (2014). "Consórcio antiferrugem: uma parceria público-privada de sucesso". In: Congresso Brasileiro de Fitopatologia. 47º Simpósio Brasileiro de Mofo Branco. Embrapa.

[38] Grecchi, R. C., Bertani, G., Trabaquini, K., Shimabukuro, Y. E., Formaggio, A. R. (2016). "Análise espaço-temporal da conversão do cerrado em áreas agrícolas na região de sapezal Mato Grosso entre os anos de 1981 e 2011". Revista Brasileira de Cartografia 68 (1):91-107.

[39] Grego, C. R., Speranza, E. A., Rodrigues, C. A. G., Nogueira, S. F., Da Silva, G. B. S., Ciferri, R. R., Luchiari Junior, A. (2019). "Definição de zonas de manejo em cana-de-açúcar usando séries temporais de NDVI derivados do Satélite Sentinel-2A". In: XIX Simpósio Brasileiro de Sensoriamento Remoto. Santos, Brasil. April 14-17.

[40] IBGE, Instituto Brasileiro de Geografia e Estatística. (2016). Levantamento Sistemático da Produção Agrícola. LSPA. IBGE.

[41] IBGE, Instituto Brasileiro de Geografia e Estatística. (2017). Censo Agropecuário 2017. Rio de Janeiro. Ministério do Planejamento. Desenvolvimento e Gestão 7:1-108.

[42] INCRA, Instituto Nacional de Colonização e Reforma Agrária. (2018). Estatísticas Cadastrais. Estrutura Fundiária Brasil. Brasília. Ministério da Agricultura.

[43] INPE, Instituto Nacional de Pesquisas Espaciais. (2020). CANASAT: Monitoramento de Cana-de-açúcar via imagens de satélite. INPE.

[44] Jensen, J. R. (2009). Sensoriamento remoto do ambiente: Uma perspectiva em recursos terrestres. São José dos Campos: Parêntese.

[45] Khanna, N., Solanki, P. (2014). "Role ofagriculture in the global economy". 2nd International Conference on Agricultural & Horticultural Sciences. Hyderabad, India. Agrotechnol. 2:4. doi:10.4172/2168-9881.S1.008.

[46] Lalmuanawma, S., Hussain, J., Chhakchhuak, L. (2020). "Applications of machine learning and artificial intelligence for Covid-19 (SARS-CoV-2) pandemic: A review". Chaos, Solitons and Fractals. doi: 10.1016/j.chaos.2020.110059.

[47] Liu, W. T. H. (2015). Aplicações de Sensoriamento Remoto. Oficina de Textos.

[48] Liu, Y., Chen, X., Wang, Z., Wang, Z. J., Ward, R. K., Wang, X. (2018). "Deep learning forpixel-level image fusion: Recent advances and future prospects". Information Fusion 42: 158-173. doi: 10.1016/j.inffus.2017.10.007.

[49] Lourenço, R. W., Landim, P. M. B. (2004). "Estudo da variabilidade do "índice de vegetação por diferença normatizada /NDVI" utilizando krigagem indicativa". HOLOS Environment 4 (1):38-55. doi:10.14295/holos.v4i1.398.

[50] Lousada, L. L., Muniz, R. A., Silva, R. M. (2012). "Variações do albedo. NDVI e SAVI durante um ciclo da cana-de-açúcar no Norte Fluminense". Revista Brasileira de Ciências Agrária 7 (4): 663-670. doi:10.5039/agraria.v7i4a1597.

[51] Lu, D., Mausel, P., Brondizio, E., Moran, E. (2004). "Change Detection Techniques". International Journal of Remote Sensing 25 (12): 2365-2407. doi: 10.1080/0143116031000139863.

[52] Lu, D., Li., G., Moran, E. (2014). "Current situation and needs of change detection techniques". International Journal of Image and Data Fusion 5 (1): 13-38. doi: 10.1080/19479832.2013.868372.

[53] MAPA, Ministério da Agricultura. Pecuária e Abastecimento. (2019). Projeções do Agronegócio. Brasil. 2018/2019 a 2028/2029. Projeções de Longo Prazo.

[54] Martinelli, L. A., Joly, C. A., Nobre, C. A., Sparovek, G. (2010). "A falsa dicotomia entre a preservação da vegetação natural e a produção agropecuária". Biota Neotropica 10 (4): 323-330. doi: 10.1590/S1676-06032010000400036.

[55] Moreira, M. A. (2011). Fundamentos de Sensoriamento Remoto e Metodologias de Aplicação. Minas Gerais: Editora UFV.

[56] Minchio, C. A., Canteri, M. G., Fantin, L. H., Silva, M. A. D. A. (2016). "Epidemias de ferrugem asiática no Rio Grande do Sul explicadas pelo fenômeno ENOS e pela incidência da doença na entressafra". Summa Phytopathologica 42 (4): 321-326. doi: 10.1590/0100-5405/2219.

[57] Nelson, R. F. (1982). Detecting forest canopy change using Landsat: final report Greenbelt: Goddard Space Flight Centre. NASA.

[58] Nunes, L. F., Lopes, C. D. S., Souza, C. C. D. (2019). "Aplicação de Lógica Fuzzy em Imagens de Satélites par a Previsão da Produção de Safra de Grãos". In: Seminário de Pesquisa e Pós Graduação Stricto Sensu. Mato Grosso do Sul, Brasil, August 14-16.

[59] OECD-FAO. (2020). Organization for Economic Co-operation and Development and the Food and Agriculture Organization. Agricultural Outlook 2020-2029. Paris: OECD Publishing, 2020. doi: 10.1787/19991142.

[60] ONU, United Nations. (2012). Department of economic and social affairs The United Nations, Population Division, Population Estimates and Projections Section.

[61] ONU, United Nations. (2015). World Water Development Report2015: Water for a Sustainable World. WWAP (United Nations World Water Assessment Programme). The United Nations, Paris, UNESCO.

[62] Onyiriuba, L., Okoro, E. O., Ibe, G. I. (2020). Strategic government policies on agricultural financing in African emerging markets. Agricultural Finance Review.

[63] Ortiz, B, Shaw, J. N. (2011). Alabama Cooperative Extension System. Alabama A&M University and Auburn. Basics of Crop Sensing.

[64] Pang, G., Wang, X., Yang, M. (2017). "Using the NDVI to identify variations in. and responses of vegetation to climate change on the Tibetan Plateau from 1982 to 2012". Quaternary International 444: 87-96. doi: 10.1016/j.quaint.2016.08.038.

[65] Pessoa, S. P., Galvanin, E. A. D., Kreitlow, J. P., Neves, S. M., Nunes, J. R., Zago, B. W. (2013). "Análise espaço-temporal da cobertura vegetal e uso da terra na Interbacia do Rio Paraguai Médio-MT, Brasil". Revista Árvore 37 (1): 119-128. doi: 10.1590/S0100-67622013000100013.

[66] Pettorelli, N., Vik, J. O., Mysterud, A., Gaillard, J. M., Tucker, C. J., Stenseth, N. C. (2005). "Using the satellite-derived NDVI to assess ecological responses to environmental change". Trends in Ecology & Evolution 20 (9): 503-510. doi: 10.1016/j.tree.2005.05.011.

[67] Pinheiro, L. C., Gomes, R. A. T., De Carvalho Junior, O. A., Guimarães, R. F., De Oliveira, S. N. (2016). "Mudanças do uso da terra e fragmentação da paisagem no município de Correntina (BA) durante 1988-2008". Raega-O Espaço Geográfico em Análise 35:169-198.

[68] Planetlabs. (2016). Planet Imagery Product Specification: PlanetScope & Rapideye. Planetlabs.

[69] Ponzoni, F. J, Shimabukuro, Y. E. (2007). Sensoriamento Remoto no Estudo da Vegetação. São Paulo: Parêntese Editora.

[70] Ribeiro, M. C., Metzger, J. P., Martensen, A. C., Ponzoni, F. J., Hirota, M. M. (2009). "The Brazilian Atlantic Forest: how much is left. and how is the remaining forest distributed? Implications for conservation". Biological Conservation 142 (6): 1141-1153. doi: 10.1016/j.biocon.2009.02.021.

[71] Ribeiro, E. P., Nóbrega, R. S., Mota Filho, F. O., Moreira, E. B. (2016). "Estimativa dos índices de vegetação na detecção de mudanças ambientais na bacia hidrográfica do rio Pajeú". Geosul 31 (62): 59-92. doi: 10.5007/2177-5230.2016v31n62p59.

[72] Rodrigues, J., Andrade, E. M., Chaves, L. C. G., Arraes, F. D. D. (2009). "Avaliação da dinâmica da cobertura vegetal na bacia Forquilha. Ceará. Brasil pelo uso do NDVI". In: XIV Simpósio Brasileiro de Sensoriamento Remoto. Natal-RN, Brasil, April 25-30.

[73] Rudorff, B. F. T., Aguiar, D. A., Silva, W. F., Sugawara, L. M., Adami, M., Moreira, M. A. (2010). "Studies on the rapid expansion of sugarcane for ethanol production in São Paulo State (Brazil) using Landsat data". Remote Sensing 2 (4): 1057-1076. doi: 10.3390/rs2041057.

[74] Scolari, D. (2009). Produção agrícola mundial: o potencial do Brasil. 2009.

[75] Sharma, H., Jain, J. S., Bansal, P., Gupta, S. (2020). "Feature Extraction and Classification of Chest X-Ray Images Using CNN to Detect Pneumonia". In: 10th International Conference on Cloud Computing. Data Science & Engineering (Confluence). IEEE, 227-231.doi: 10.1109/Confluence47617.2020.9057809

[76] Shimabukuro, Y. E., Novo, E. M. N., Ponzoni, F. J. (1998). "Índice de Vegetação e Modelo Linear de Mistura Espectral no Monitoramento da região do Pantanal". Pesquisa Agropecuária Brasileira 33 (1): 1729-1737.

[77] Silva, L. F. (2017). "Detecção de mudanças e modelagem preditiva do uso da terra e cobertura vegetal do pantanal de Aquidauana". Dissertação de Mestrado em Geografia, Universidade Federal de Mato Grosso do Sul.

[78] Sousa, R., Marques, O., Sene Jr, I. I. G., Soares, A., De Oliveira, L. L. (2013). "Comparative performance analysis of machine learning classifiers and dimensionality reduction algorithms in detection of childhood pneumonia using chest Radiographs". Procedia Computer Science 18: 2579-2582. doi: 10.1016/j.procs.2013.05.444.

[79] Svetlana, P., Irena, J., Zaklina, S. (2018). The importance of bank credits for agricultural financing in Serbia. 65(1).

[80] Teotia, H. S., Silva, I. F., Santos, J. R., Veloso Junior, J. F., Gonçalves, J. L. G. (2003). "Classificação da cobertura vegetal e capacidade de uso da terra na região do Cariri Velho (Paraíba). através de sensoriamento remoto e geoprocessamento". In: XI Simpósio Brasileiro de Sensoriamento Remoto. Belo Horizonte, Brasil, 1969-1976, April 05-10.

[81] Tewkesbury, A. P., Comber, A. J., Tate, N. J., Lamb, A., Fisher, P. F. (2015). "A Critical Synthesis of Remotely Sensed Optical Image Change Detection Techniques". Remote Sensing of Environment 160 (1): 1-14. doi: 10.1016/j.rse.2015.01.006.

[82] Vallat, R. 2018. "Pingouin: Statistics in Python". Journal of Open Source Software 3 (31): 1026. doi: 10.21105/joss.01026.

[83] Wanga, Q., Chena, J., Tiana, Y. (2008). "Remote sensing image interpretation study serving urban planning based on GIS". In: XXXVII International Archives of the Photogrammetry. Remote Sensing and Spatial Information Sciences. Beijing. China. 453-456.

[84] Zhang, H. (2009). Comparison of Investment and Financing Systems in Foreign Agriculture and Their Enlightenments for China. Asian Social Science.

[85] Zhang, P., Gong, M., Su, L., Liu, J., Li, Z. (2016). "Change detection based on deep feature representation and mapping transformation for multi spatial resolution remote sensing images". ISPRS Journal of Photogrammetry and Remote Sensing. 116: 24-41. doi: 10.1016/j.isprsjprs.2016.02.013.